



Research paper

An Assessment of the impacts of selected Meteorological and Land Use Land Cover Datasets on the accuracy of wind speeds downscaled with the Weather Research and Forecasting Model for coastal areas in Ghana

Denis Edem K. Dzebre^{a,b,*}, Charlotte Asiedu^a, Eric Akowuah^a, Samuel Boahen^a, Kofi O. Amoabeng^a, David Oppong^a

^a *Department of Mechanical Engineering, Kwame Nkrumah University of Science and Technology, Kumasi, Ghana.*

^b *The Brew Hammond Energy Centre, Kwame Nkrumah University of Science and Technology, Kumasi, Ghana.*

ARTICLE INFO

Article history:

Received February 13, 2024

Accepted June 27, 2024

Keywords:

WRF,
Wind resources,
Assessment,
Analysis and reanalysis
datasets,
Land use and land cover
datasets,
Wind energy.

ABSTRACT

Downscaling of wind speeds with the Weather Research and Forecasting model (WRF) model requires inputs from datasets such as Meteorological and Land Use and Land Cover (LULC) datasets. The accuracy of these datasets is among the factors that significantly impact the accuracy of the wind speeds that are generated by the model. In this study, we assess the accuracy of wind speeds data that are downscaled for an area in coastal Ghana using six meteorological, and two global Land use and Land Cover (LULC) datasets as inputs to the WRF model. In contrast to the LULC datasets tested, model wind speeds for the area were more significantly impacted by the different meteorological datasets. Meteorological datasets that were produced with higher resolution forecasts combined with more advanced data assimilation techniques produced better estimates of wind speed, and vice versa. The JMA JRA55 Reanalysis, NCEP GFS Analysis data, and ECWMF ERA5 gave the relatively best combinations of wind speed error metrics and are therefore recommended for consideration for downscaling of wind speeds for wind resources assessment in the coastal regions of Ghana. However, the ECWMF ERA5 is preferred as its mean error margins are fairly constant and so should be easier to correct.

1. INTRODUCTION

Global energy consumption has always been on the increase in response to industrialization and rising living standards among other factors. The quest for sustainable ways of meeting this demand has

* *Corresponding author, E-mail address: dek.dzebre@yahoo.com*



generated interest in renewable sources of energy, such as wind. Wind energy, harnessed from the kinetic energy in naturally moving air across the earth's surface offers a clean, inexhaustible, and increasingly cost-effective alternative to fossil fuels (Breeze, 2019). The cost-competitiveness of wind power continues to improve, and with increasing capacity from established and emerging markets, total wind capacity is expected to reach over 2 TW by 2030 from the 906 GW in 2023 (Global Wind Energy Council, 2023).

Due to the geographical and temporal variability of wind, thorough assessments are necessary to determine the viability of power projects. Pre-feasibility assessments are essential in the process and involve broad area screenings for potential wind power sites, designing effective mast measurement campaigns, and assessing project feasibility. These prefeasibility assessments, have traditionally been done with data from mast mounted instruments, and in recent times, remote sensors such as Light Detection and Ranging (LIDAR) and Sound Detection and Ranging (SODAR). However, owing to the time consuming and the expensive nature of measuring campaigns with such instruments, an alternatively increasingly popular source of data for these assessments is downscaled meteorological datasets, often created using Numerical Weather Prediction (NWP) models. NWP models, such as the Weather Research and Forecasting (WRF) model, are often used for this downscaling process. In a process referred to as dynamical downscaling, these models modify initial conditions (from the meteorological datasets) to predict time varying atmospheric data for points on a simulation grid, to generate data for desired locations and whole areas of interest (Warner, 2011). The process takes into account several factors, which include the land cover and topographical properties of the area for which the data is desired (Jiménez-Esteve, Udina, Soler, Pepin, & Miró, 2017). The land cover and topographical properties serve as inputs in the calculation of heat and energy fluxes which affect turbulence, which acts as a feedback mechanism in wind circulation in the atmosphere (Jiménez-Esteve et al., 2017). Therefore, in addition to other factors (such as the parameterisation of the processes occurring on the sub-grid scale), the accuracy of the surface properties, the meteorological datasets (which provide initialisation and driving data), can significantly impact the quality of the data generated from the downscaling process (Fernández-González et al., 2017; Zhao & Wu, 2018). This paper focuses on these input datasets.

The meteorological datasets are often Analysis and Reanalysis datasets. They are produced via data assimilation, a process that involves the provision of a forecast of the atmosphere, which is updated in light of observations (Parker, 2016; Warner, 2011). Reanalysis datasets are produced with a frozen system (forecast models and data assimilation methods) that remains unchanged over the temporal coverage (or range) of the dataset. The systems for producing Analysis datasets on the other hand benefit from model updates and upgrades over time (D. Dee, Fasullo, Shea, Walsh, & 2016; D. P. Dee et al., 2011; Warner, 2011). In addition, unlike Analysis datasets, Reanalysis datasets assimilate data from past periods, using a current model to produce a long-term, model-consistent dataset (Parker, 2016). Differences in the (capabilities of the) forecast models and data assimilation techniques, as well as the amount and quality of the raw observational data that are used in their production, introduce unavoidable differences in the quality of initialisation datasets and their impacts on hindcasted data (D. Dee et al., 2016; McGuffie & Henderson-Sellers, 2005; Warner, 2011).

Moisture and heat fluxes at the lower levels of the atmosphere, are essential for better hindcasts of surface winds by NWP. Planetary Boundary Layer (PBL) parameterisation schemes in the WRF model need surface terrain parameters, such as surface roughness length, albedo, moisture, and emissivity, among others, serve as inputs in the estimation of these fluxes (Boadh, Satyanarayana, Rama Krishna, & Madala, 2016). They are calculated by the surface layer parameterization schemes in the WRF model, from tabulated values associated with different Land Use and Land Cover (LULC) category datasets which serve as sources of data on surface properties in WRF simulations (Santos-Alamillos, Pozo-

Vázquez, Ruiz-Arias, & Tovar-Pescador, 2015). Different (meteorological and LULC) datasets have been found to have varying impacts on hindcasted wind speeds for different areas (Carvalho, Rocha, Gómez-Gesteira, & Silva Santos, 2014; Chadee, Seegobin, & Clarke, 2017; De Meij & Vinuesa, 2014; Ghati & Mohan, 2015; Mughal et al., 2017; Santos-Alamillos et al., 2015; Yang & Duan, 2016; Zhao & Wu, 2018).

The fast population expansion and ambitious development plans of Ghana is progressively increasing the country's need for power, something that continues to prove to be a challenge for the power sector of the country. A National Energy Transition Framework which is expected to complement efforts at increasing renewable energy penetration in the country's energy mix, was launched in recent years. A Renewable Energy Masterplan policy document (Ghana Renewable Energy Master Plan Taskforce, 2019), which is to help in this regard, identified the need for more and improved assessments of resources such as wind, to aid better planning for the overall development in country's renewable energy sector. In view of the role downscaling tools can play in this regard, in the past couple of years, there has been several studies (Dzebre, Acheampong, Ampofo, & Adaramola, 2019; Dzebre & Adaramola, 2019; Dzebre, Ampofo, & Adaramola, 2021) aimed at optimizing the WRF model for the downscaling of wind data for mapping and generating of time series data for such prefeasibility assessments. While they have focused on several important aspects of the model, namely the Planetary Boundary Layer and Surface Layer parameterization schemes (Dzebre & Adaramola, 2019), simulations run time length and nudging options (Dzebre et al., 2019), and effects of total length of periods simulated in studies (Dzebre et al., 2021), none of them or any other studies from open literature has assessed the impact of the datasets that are downscaled on the accuracy of the wind data produced for the country Ghana. Against this background, this paper assesses the impact of selected meteorological and LULC datasets on surface wind speeds for an area on the coast of Ghana. The paper aims to offer an insight into how wind speeds that are hindcasted with the WRF model for this area in Ghana, vary with respect to six selected meteorological, as well as two LULC datasets.

2. DATA AND METHODS

2.1 Study Area, Data and Model Configuration

The study area covers the coastal plains of south east Ghana. Seasonal variations and the topography in the area have been well described in previous studies by Dzebre and Adaramola (2019). The measured wind data for this study was measured on a mast (5.786 °N, 0.918 °E) at Anloga in a wind measurement campaign by the Energy Commission of Ghana. The data comprises wind speeds at heights of 40 m, 50 m, and 60 m above ground level.

The Advanced Research WRF (ARW) 3.8.1 was used for this study. A detailed description of key model features, physics, equations and dynamics is provided by (Skamarock, 2008). The simulation domains and model configuration presented in Figure 1 and Table 1 respectively, are from the prior WRF sensitivity studies (Dzebre et al., 2019; Dzebre & Adaramola, 2019) for this area of Ghana.

The candidate meteorological datasets were Gridded Binary (GriB) datasets selected from the Research Data Archive (RDA) of the National Centre of Atmospheric Research (NCAR) ("WRF Users Page: Available GRIB Datasets from NCAR," 2020), and the Copernicus Climate Database (Hersbach, 2018). These are the;

- i) NCEP Climate Forecast System Version 2 (Saha et al., 2011),
- ii) ECMWF ERA 5 (ERA 5) (Hersbach, 2018),
- iii) ECMWF ERA Interim (ERA-I) (ECWMF, 2012),
- iv) NCEP Final Analysis (GFS-FNL) (National Centers for Environmental Prediction/National Weather Service/NOAA/U.S. Department of Commerce, 2000a),

- v) JMA JRA-55 (JRA55) (Japan Meteorological Agency, 2013), and the
- vi) NCEP/DOE R2 (R2) (National Centers for Environmental Prediction/National Weather Service/NOAA/U.S. Department of Commerce, 2000b).

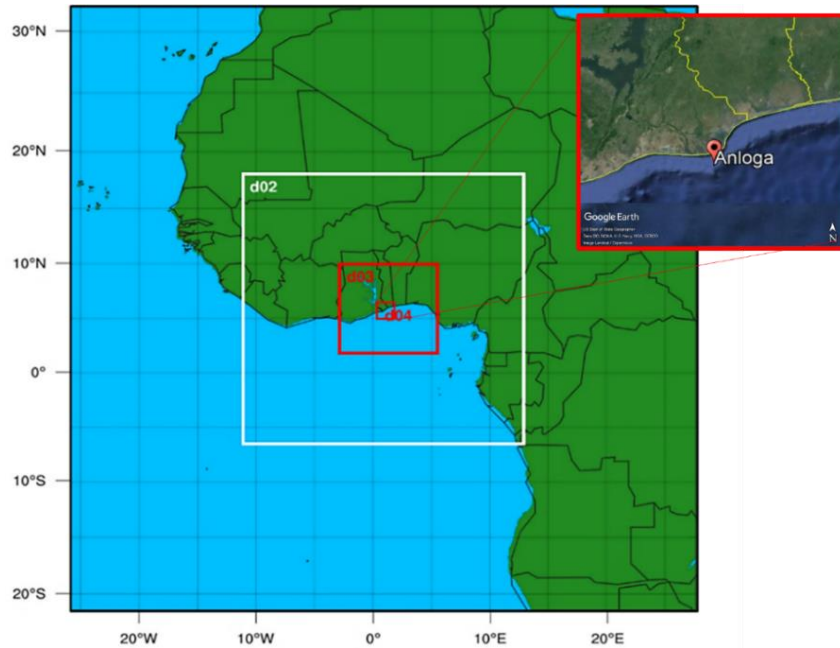


Fig 1: Simulation domains.

Selected characteristics of the meteorological datasets (as tested) are summarised in Table 2. Datasets that did not cover the period for which we had observational data for verification or had been improved upon by another dataset (as was the case with the NCEP/NCAR R1) were not tested.

Table 1: Model Configuration

Model Version	Advanced Research WRF v3.8.1			
Candidate Meteorological (driving) datasets	<ul style="list-style-type: none"> i) NCEP CFS version 2 (CFSv2) ii) ECMWF ERA 5 (ERA 5) iii) ECMWF ERA Interim (ERA-I). iv) NCEP Final Analysis (GFS-FNL). v) JMA JRA-55 (JRA55). vi) NCEP/DOE R2 (R2). 			
Topographical data	USGS GMTED2010			
Candidate LULC datasets	<ul style="list-style-type: none"> i) MODIS with lakes ii) USGS with lakes 			
Vertical Resolution	40 vertical levels (automatically set), model top 50 hPa			
Domains	d01	d02	d03	d04
Horizontal resolution (km)	81	27	9	3
Domain size (grid points)	74 x 77	100 x 103	103 x 103	65 x 65
Parameterization Schemes:	As recommended by Dzebre et al. (2019) for coastal areas in Ghana.			

The candidate LULC datasets are the two default global LULC datasets that come with WRF v3.8.1 ("WRF V3 Geographical Static Data Downloads Page Page,"). The United States Geological Survey (USGS) LULC dataset takes its primary inputs from composite images from the Advanced Very High-Resolution Radiometer (AVHRR) satellite, sourced from April 1992 to March 1993 (Schicker, Arnold Arias, & Seibert, 2016). It has 24 land cover categories, classified according to the Normalised Difference Vegetation Index (NDVI) (Schicker et al., 2016). The Moderate Resolution Imaging Spectroradiometer (MODIS) LULC dataset on the other hand is derived from data from the Terra/Aqua

Earth Observation System satellites, and has 20 land cover classes, as defined by the International Geosphere Biosphere Program (IGBP) (Schicker et al., 2016). Both LULC datasets were tested in combination with the special land cover dataset in the WRF model that distinguishes between oceans and inland water bodies (lakes) (Wei Wang, 2016). Plots of the categories from both datasets (for simulation domain 2) are shown in Figure 2. The MODIS LULC plot has been reclassified to USGS according to (Schicker et al., 2016) for easier comparison.

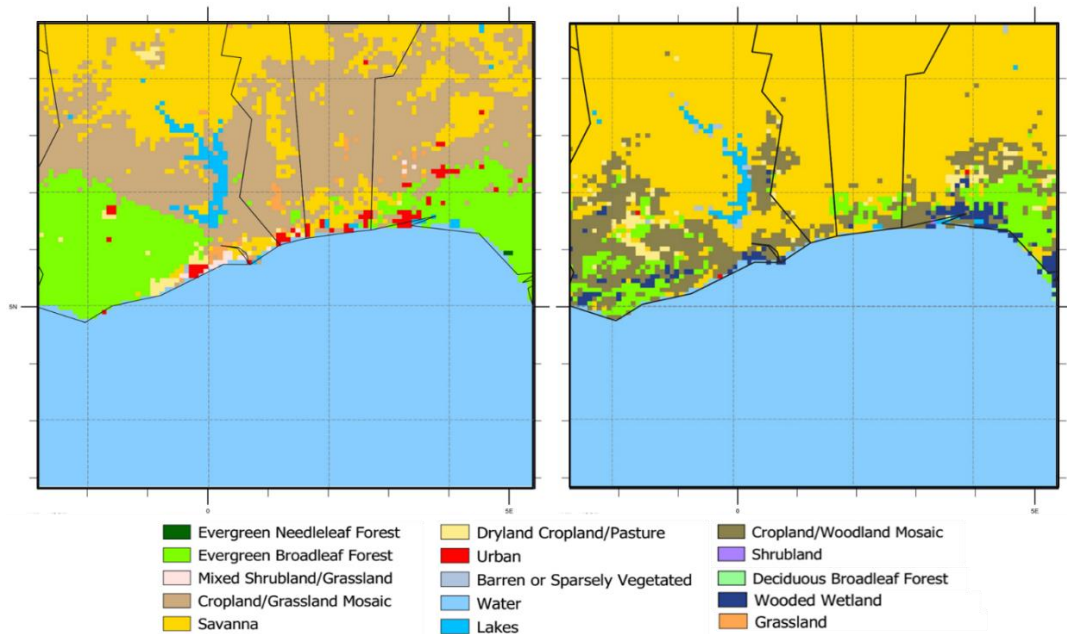


Fig 2: Plot of the reclassified MODIS (left) and USGS (right) LULC in the Second Domain.

Table 2: Selected specifications of initialisation and driving datasets tested (D. Dee et al., 2016)

Dataset	Data Type	AGCM* Resolution	Data Assimilation Technique	Resolution tested (lon. x lat. x pressure levels)
CFSv2	Reanalysis	T126, L64 0.266 hPa top	3DVAR	0.5 x 0.5 x 37
ERA5	Reanalysis	T636, L137 0.01 hPa top	4DVAR	0.25 x 0.25 x 37
ERA-I	Reanalysis	T255, L60 0.1 hPa top	4DVAR	0.703 x ~0.702 x 37
GFS-FNL	Analysis	T574/T190, L64	Hybrid 3DVAR	1 x 1 x 26
JRA55	Reanalysis	T319, L60 0.1 hPa top	4DVAR	1.25 x 1.25 x 37
R2	Reanalysis	T62, L28 3 hPa top	3DVAR	2.5 x 2.5 x 18

* Atmospheric Global Circulation Model

2.2 Experimental Design

Twelve experiments were conducted. In each experiment, wind speeds were hindcasted for February and September 2013. The two months were carefully selected from the two seasons in the area as described by (Dzembre & Adaramola, 2019) in a test approach that has been previously used in wind sensitivity studies (Dzembre et al., 2019; Dzembre & Adaramola, 2019) for coastal areas in Ghana. This approach of testing representative months from the two main seasons in the area, has been found to result in acceptable conclusions for the area when conclusions are based on an evaluation of consistency in performance of tested options across multiple evaluation criteria, and preset performance benchmarks (Dzembre et al., 2021). Each of the 12 experiments tested a different LULC and meteorological dataset pair. Details of the dataset pairings are presented in Table 3. The JRA55 dataset had to be complemented with soil data from the GFS-FNL dataset for the JRA55 experiments, as its initial runs were not successful. The nudging technique in the WRF model's Data Assimilation (WRFDA) System was

applied in each simulation as recommended by Dzebre et al. (2019), with a simulation run time of 30 days and a model spin up time of 12 hours. The R2 experiments were run with all four domains, due to its relatively rough spatial resolution, while the ERA5 experiments were run with just the 2 inner domains due to its relatively finer spatial resolution.

Table 3: Experimental Design

	Experiment Name	Initialization Data	LULC Data	Domains Used
1	MODIS_CFSv2	NCEP CFSv2	MODIS	d02, d03, d04
2	MODIS_ERA5	ECWMF ERA 5	MODIS	d03, d04
3	MODIS_ERA-I	ECWMF ERA Interim	MODIS	d02, d03, d04
4	MODIS_FNL	NCEP GFS FNL	MODIS	d02, d03, d04
5	MODIS_JRA55	JMA JRA55	MODIS	d02, d03, d04
6	MODIS_R2	NCEP/DOE R2	MODIS	d01, d02, d03, d04
7	USGS_CFSv2	NCEP CFSv2	USGS	d02, d03, d04
8	USGS_ERA5	ECWMF ERA 5	USGS	d03, d04
9	USGS_ERA-I	ECWMF ERA Interim	USGS	d02, d03, d04
10	USGS_FNL	NCEP GFS FNL	USGS	d02, d03, d04
11	USGS_JRA55	JMA JRA55	USGS	d02, d03, d04
12	USGS_R2	NCEP/DOE R2	USGS	d01, d02, d03, d04

2.2 Post-processing and Evaluation of Results

Post-processing of predictions followed the procedure that has been used in previous optimization studies (Dzebre et al., 2021) for Ghana; bilinear interpolation of the simulated wind speeds from the four closest grid points in domain 4 was used to obtain the simulated wind speeds for the mast location. Simulated wind speeds for the heights of analysis (40 m, 50 m, and 60 m), were obtained from the the two closest half vertical levels (which were at approximately 28 m and 69 m agl) using log-linear interpolation as formulated by Deserno (2004). Assessment followed the same techniques used in previous studies (Dzebre et al., 2019; Dzebre & Adaramola, 2019; Dzebre et al., 2021) for coastal Ghana. Error metrics, namely Root Mean Square Error (RMSE), Mean Error (ME), Standard Deviation of the Error (STDE) and Correlation Coefficient (CC) between simulated and observed wind speeds were evaluated and compared to performance benchmarks (RMSE < 2 m/s, ME < +0.5 m/s. CC > 0.7) as used by Emery, Tai, and Yarwood (2001); Gunwani and Mohan (2017) and Mughal et al. (2017) in similar studies and the already mentioned WRF optimization studies on coastal Ghana. In addition, to the performance benchmarks, the error metrics were combined into a Prediction Skill Score (SS) based on which the tested combinations of datasets were ranked. The Weibull Cumulative Density functions of simulated and observed wind speeds were also compared via the absolute Cumulative Distribution Function Error (Max CDF Error). Furthermore, the mean Wind Power Densities (WPD) from the simulated data was also compared to those from observed data in terms of a percentage error. All the metrics were calculated with the same formulations as has been used in the previous optimization studies for Ghana as follows;

Root Mean Squared Error,

$$RMSE = \sqrt{\left(\frac{1}{N} \sum_i^N (v_{sim} - v_{obs})^2\right)} \quad (1)$$

Mean Error,

$$ME = \frac{1}{N} \sum_i^N (v_{sim} - v_{obs}) \quad (2)$$

where N is the number of data points, v_{sim} is the downscaled/simulated wind speed, and v_{obs} is observed or measured wind speed.

Standard Deviation of the Error,

$$STDE = \sqrt{(RMSE^2 - ME^2)} \quad (3)$$

Correlation Coefficient,

$$CC = \frac{\sum(v_{sim} - \bar{v}_{sim})(v_{obs} - \bar{v}_{obs})}{\sqrt{\sum(v_{sim} - \bar{v}_{sim})^2 \sum(v_{obs} - \bar{v}_{obs})^2}} \quad (4)$$

Prediction Skill Score,

$$SS = (1 - RMSE_{NORMALIZED}) + (1 - |ME|_{NORMALIZED}) + (1 - |STDE|_{NORMALIZED}) + (CC_{NORMALIZED}) \quad (5)$$

such that $0 \leq Skill\ Score \leq 4$ and the dataset pair with the highest skill score was ranked as the best and vice versa. Each metric was normalized (scaled) to read between 0 and 1 according to the method of Gbode, Dudhia, Ajayi, and Ogunjobi (2017);

$$X_{NORMALIZED} = \frac{X_i - X_{min}}{X_{max} - X_{min}} \quad (6)$$

Absolute Maximum CDF Error,

$$|Max\ CDF\ Error| = \max|F(v_i)_{obs} - F(v_i)_{sim}| \quad (7)$$

where the Cumulative Distribution, $F(v)$ is given by

$$F(v) = 1 - \exp\left[-\left(\frac{v}{c}\right)^k\right] \quad (8)$$

where v , c and k respectively are the wind speed, Weibull scale and shape factors respectively. The scale and shape parameters were estimated using the Empirical (mean and standard deviation) method as recommended by Dzebre and Adaramola (2019) in a prior study for the area.

The Wind Power Density was determined as;

$$WPD = \left[\frac{1}{2}\rho c^3\Gamma\left(1 + \frac{3}{k}\right)\right] \quad (9)$$

where Γ is the gamma function and ρ , air density which was assumed to be 1.160 kg m^{-3} , as estimated in a previous study for coastal Ghana (Dzebre et al., 2019).

3. RESULTS

Averages of observed and downscaled wind speeds, and evaluation metrics at 60 m for the 2 months modelled are presented in Table 4. The variation of hourly average wind speeds diurnally for each Meteorological dataset paired with both LULC datasets is also presented in Figure 3. It can be seen from the Table that, metrics of the MODIS LULC did not differ greatly from those of the USGS LULC, irrespective of the meteorological dataset it was paired with. Differences in wind speeds were less than

0.2 m/s in all cases. The similarity in wind speeds with respect to the two LULC datasets can also be seen in the diurnal wind speed profiles shown in Figure 3. In addition, for each meteorological dataset, though the wind speeds after sunset were slightly more different for some of the datasets, this difference was often much less during the day. The MODIS LULC produced relatively higher wind speeds between 00:00 hrs and 06:00 hrs, and relatively lower wind between noon and sunset. However, the margins of difference varied among the meteorological datasets.

In contrast to the LULC datasets, average wind speeds and error metrics differed relatively more significantly among the meteorological datasets tested. Most of the meteorological datasets met the RMSE and CC benchmarks for performance (i.e. $RMSE < 2.0$ m/s, $CC \geq 0.7$). However, the CC of the CFSv2 was less than required, and all the metrics of the NCPE/DOE R2 did not meet any of the benchmarks. None of the datasets met the benchmark for ME. However, the JRA55 had the relatively least absolute ME. While the CC of the ERA5 was best, followed closely by that of the GFS-FNL dataset. Irrespective of LULC, the JRA55 had the best combination of metrics followed by the GFS-FNL and the ERA5, while the R2 had the relatively worst combination of metrics. In terms of the wind speed profiles, the ERA5 appears to best replicate the profile of the mast observations, with error margins though quite large, being quite constant all day. However, compared to the ERA5, the JRA55 gave relatively better error margins overall.

Table 4: Average predictions and Statistical Metrics at 60 m for the entire study period.

Experiment	Average Wind Speeds (m/s)	RMSE (m/s)	STDE (m/s)	CC	ME (m/s)	Skill Score
Observation	6.89					
MODIS_CFSv2	6.11	1.64	1.17	0.63	-0.78	2.45
USGS_CFSv2	6.10	1.65	1.45	0.64	-0.79	2.46
MODIS_ERA5	5.77	1.62	1.17	0.77	-1.12	3.07
USGS_ERA5	5.81	1.60	1.17	0.77	-1.08	3.13
MODIS_ERA-I	5.82	1.68	1.29	0.72	-1.07	2.62
USGS_ERA-I	5.74	1.77	1.34	0.70	-1.15	2.21
MODIS_FNL	6.00	1.49	1.20	0.76	-0.89	3.44
USGS_FNL	5.94	1.52	1.19	0.76	-0.95	3.37
MODIS_JRA55	6.26	1.43	1.28	0.74	-0.63	3.66
USGS_JRA55	6.22	1.46	1.30	0.73	-0.66	3.49
MODIS_R2	5.65	2.15	1.76	0.53	-1.24	0.19
USGS_R2	5.54	2.18	1.71	0.54	-1.35	0.14

Similar trends were observed on the Mean WPD, the Mean WPD Error and Max CDF Errors, as can be seen in Table 5. Though the MODIS LULC often had lower mean WPD errors, its values were often not more than 2 percentage points better than the mean WPD errors of the USGS LULC for the same meteorological dataset. Among the datasets, The JMA JRA55 again had the relatively lowest Mean WPD and Max CDF errors, while the R2 had the relatively worst. Unlike the case of the wind speeds estimates, the WPD errors for the CFSv2 were better than those for the all the datasets except the JRA55. Significant differences were not observed in the above trends in similar analyses at 50 m and 40 m (see Table A1 in the appendix).

In seasonal evaluations presented in Table A2 in the Appendix, the JRA55, FNL, and the ERA5 datasets again, largely remained the best three datasets in terms of Skill Score irrespective of season. Though the maximum CDF errors of the R2 improved in the seasonal analyses, its wind speed error metrics were still often the worst among the other datasets.

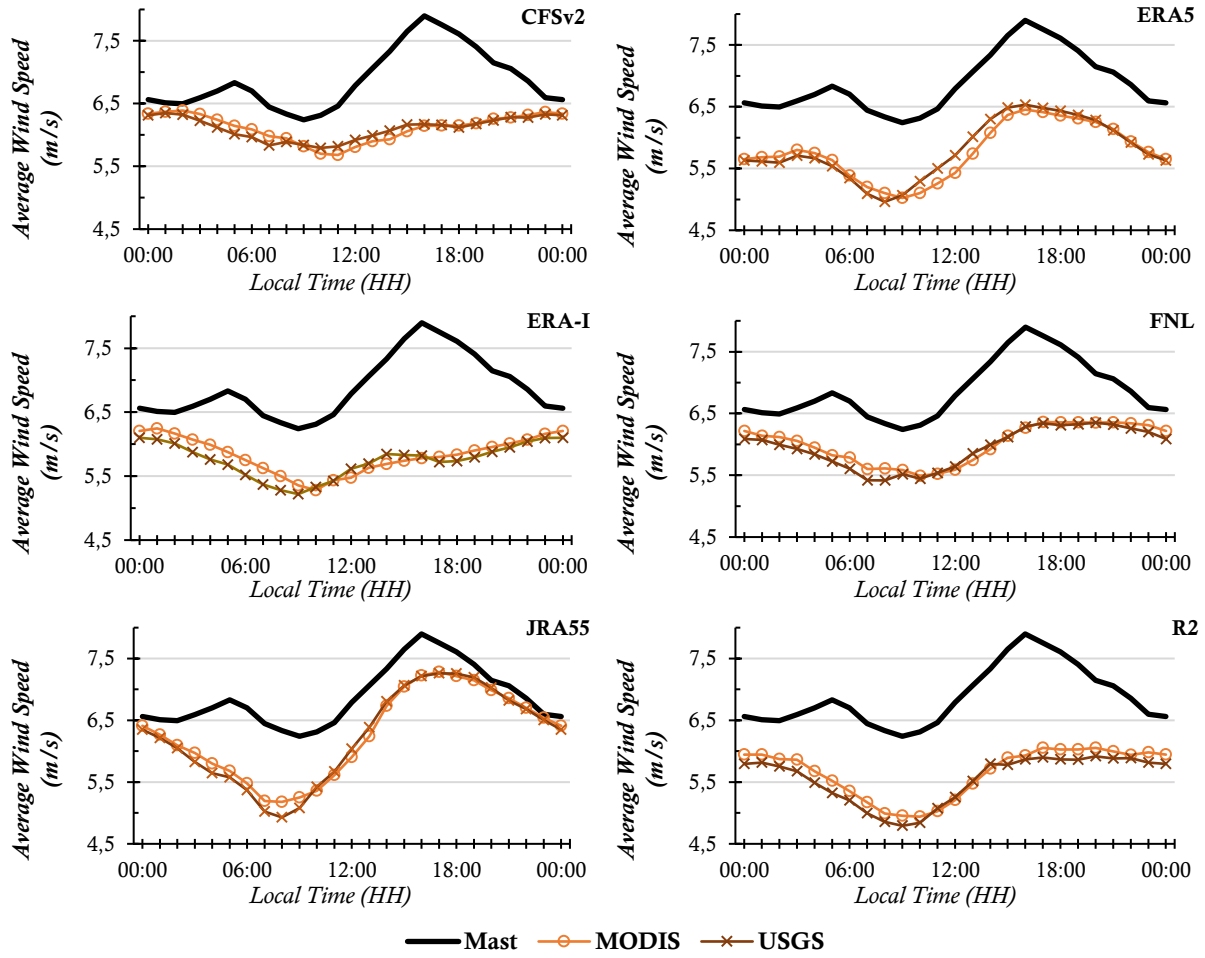


Fig 3: Comparison of the diurnal wind speeds for each Meteorological dataset paired with both LULC datasets.

Table 5: Weibull parameters, Mean WPD Error, and Max CDF Errors.

	c	k	Mean WPD (Wm ⁻²)	Mean WPD Error (%)	Max CDF Error
Observation	7.6	4.2	230	0	0
MODIS_CFSv2	6.7	4.9	153	-33.4	0.22
USGS_CFSv2	6.7	4.7	154	-33.1	0.21
MODIS_ERA5	6.3	4.3	134	-41.6	0.27
USGS_ERA5	6.4	4.4	136	-41.1	0.27
MODIS_ERA-I	6.4	4.3	138	-40.1	0.26
USGS_ERA-I	6.3	4.2	133	-42.3	0.28
MODIS_FNL	6.6	4.8	147	-36.3	0.23
USGS_FNL	6.5	4.7	143	-38.1	0.25
MODIS_JRA55	6.9	4.2	173	-24.9	0.15
USGS_JRA55	6.9	4.1	171	-25.9	0.15
MODIS_R2	6.3	3.5	136	-41.0	0.27
USGS_R2	6.2	3.5	128	-44.5	0.29

4. DISCUSSION

The quality of downscaled data depends on a combination of several factors which include the quality of the input datasets and the capabilities of the downscaling model itself. It will be difficult to

satisfactorily explain trends in our results without considering all these factors and how they interact with each other to affect the final downscaled data. Nonetheless, some of the trends in the comparisons of the initialisation datasets can be explained to some extent.

The meteorological datasets can be classified according to some key characteristics, which include; the type of dataset (whether analysis or reanalysis), the data assimilation technique that was used in the (analysis/reanalysis) process, the type of AGCM and the resolution at which it produced the forecasts for the (analysis/reanalysis) process, and the final resolution of the datasets from this process. From Table 2 which summarises these characteristics for the tested meteorological datasets, the ERA-I, ERA5 and JMA JRA55 can be classified as newer third-generation Reanalyses, with the R2, a first generation Reanalysis, in terms of data assimilation capabilities, as explained by D. Dee et al. (2016). The FNL is an analysis dataset, and the CFSv2, though a first generation reanalyses like the R2 differs from the others, in that it is a Coupled Reanalysis, utilising forecasts from a Coupled Forecast Model (a coupled atmosphere–ocean–sea ice–land model to better account for ocean interactions) in its forecasts (D. Dee et al., 2016; Saha et al., 2014).

As already discussed, data assimilation plays a major role in producing meteorological datasets. The mathematical concepts and basis for various approaches to data assimilation, are quite extensively described in texts such as (Rabier & Liu, 2003; Warner, 2011). A major advance in data assimilation came with the introduction of the variational 3DVAR method which enabled the use of worldwide observations (Warner, 2011). However, limitations of 3DVAR data assimilation include its inability to use asynoptic data (data measured at times other than the synoptic hours of 00, 06, 12 and 18 UTC) and account for the time-evolution of the errors associated with data (Huang et al., 2009; Lorenc, 2003; Rabier & Liu, 2003). The 4DVAR method tries to address this with a linear forecast model to account for the evolution of perturbations in the atmospheric state, representing and calculating the time-evolution of errors from the forecast and observational data, albeit at extra computational cost (Barker et al., 2012; Lorenc, 2003; Rabier & Liu, 2003). The Hybrid (Variational–Ensemble) data assimilation technique combines the variational data assimilation with the Ensemble Kalman Filter (EnKF) technique. The Ensemble Kalman Filter (EnKF) technique (like the 4DVAR,) addresses the time-evolution errors by deriving error estimates from nonlinear short-range forecasts from an Ensemble Prediction System (EPS) (Barker et al., 2012; Lorenc, 2003). The Hybrid data assimilation technique has been found to sometimes offer comparatively better performance over the pure variational and pure ensemble techniques in both 3DVAR and 4DVAR modes (Barker et al., 2012; Kalnay, Li, Miyoshi, Yang, & Ballabrera-Poy, 2007). The relatively better, often consistent performance of the FNL, ERA5, and JRA55 is therefore understandable, as they are newer generation datasets, produced with relatively better data assimilation techniques.

The forecast resolutions of the AGCMs employed in the production of the meteorological datasets is also of importance (D. Dee et al., 2016; McGuffie & Henderson-Sellers, 2005). The AGCMs, are basically NWP models that are often formulated with the spectral method, as opposed to finite difference method used in finite-grid models such as the WRF model by McGuffie and Henderson-Sellers (2005), who go on to explain the differences in the formulations of the two methods and how they impact model performance. A key advantage of the spectral method which might explain its wide use in AGCMs is that, it is relatively less computationally expensive (McGuffie & Henderson-Sellers, 2005). The horizontal resolution of spectral models is governed by a wavenumber of truncation (T -number), while the number of levels in the atmosphere (L -number) govern their vertical resolution (McGuffie & Henderson-Sellers, 2005). Higher T and L numbers, which are typical of the newer datasets often mean better forecasts and possibly better datasets (D. Dee et al., 2016). This is likely the reason for the often-relative worse wind speed metrics of the of the R2 and CFSv2 Reanalysis as compared to all the other datasets, as they use AGCM forecasts of relatively worse resolution.

The diminutive impact of LULC change on wind speeds observed in this study might be partly due to the proximity of the mast location to the sea, and partly due to the nature of the local winds in the studied area. As was discussed in (Dzebre & Adaramola, 2019), the local winds in the area comprise land and sea breezes. The impact of the difference LULCs should be more apparent on the (night-time) land breezes, as the winds blowing from inland areas to the sea would be influenced by the differences in the surface properties of the varying land cover types in the two LULC. Most of the diurnal wind speed profiles from Figure 3 appear to confirm this; for the same meteorological dataset, there is a larger difference in the night time and early morning wind speeds from the LULC datasets as compared to the day time winds. The relatively higher (daytime) wind speeds are probably diminishing the significance of this (night-time variation) on the overall average wind speeds. Furthermore, the already diminished influence of the surface properties on the wind speeds was probably further reduced during postprocessing, as the post-processed wind speeds (which were evaluated in this study), were interpolated from simulated wind speeds at the four closest points on the simulation grid, one of which in (our case) was a point on the surface of the sea, where there is no difference as far as the two LULC datasets are concerned (see Figure 2). Therefore, though the change of LULC datasets had little impact on the mean wind speeds and WPDs, further studies, preferably with a finer simulation grid, using verification data from locations further inland, which should address the two issues already mentioned, are warranted to properly assess the impacts of the LULC datasets on wind speeds in the area. But with the current results, the MODIS LULC appears to be predicting higher and better wind speeds.

5. SUMMARY AND CONCLUSION

Land Use and Land Cover (LULC) and meteorological datasets have been reported to have varying impacts on the quality of dynamically downscaled wind data by the WRF model worldwide (Carvalho et al., 2014; Chadee et al., 2017; De Meij & Vinuesa, 2014; Ghatai & Mohan, 2015; Mughal et al., 2017; Santos-Alamillos et al., 2015; Yang & Duan, 2016; Zhao & Wu, 2018). Against this background, this study sought to recommend LULC and GrIB formatted meteorological datasets data from the options available at ("WRF V3 Geographical Static Data Downloads Page Page,") and ("WRF Users Page: Available GRIB Datasets from NCAR," 2020) respectively on wind speeds downscaled with the WRF model for a coastal area in Ghana. The study also sought to identify characteristics of the meteorological datasets that often correlated well with good hindcasts to inform choices in future downscaling exercises or studies. Two LULC datasets and six meteorological datasets were tested in 12 dynamical downscaling experiments.

Results confirm that, the accuracy of the downscaled data depends on the meteorological datasets that are downscaled (Boadh et al., 2016; Fernández-González et al., 2017; Yang & Duan, 2016). In addition, when newer generation reanalysis meteorological datasets are downscaled, the wind speeds are better (in terms of most of the evaluation criteria considered in this study) than older generation ones (Carvalho et al., 2014; D. Dee et al., 2016). Among the meteorological datasets tested, the JMA JRA55, ECWMF ERA5 and NCEP GFS FNL gave some of best combination of error metrics, Mean Wind Power Density and Cumulative Density Function errors. But it should be noted that the Mean Errors of the are quite constant, and so its downscaled wind speeds should be easier to correct. On the LULC datasets, the MODIS LULC often gave the relatively better combination of error metrics as well as Mean WPD and CDF Errors when compared to the USGS LULC. However, evaluation metrics of the two LULC datasets were almost the same in almost all cases. Given the proximity of the location of the mast from which verification data was measured to the sea coupled with our postprocessing technique, and the nature of local winds, which we believe could have affected the wind speeds at the evaluation location, it is recommended that further studies, preferably on finer simulation grid, using verification data from

locations further inland be carried out to properly assess the impacts of the LULC datasets on wind speeds in the area. Such future tests studies should incorporate a test of Sea Surface Temperature datasets.

Therefore, it is concluded that those tests of different meteorological datasets are necessary to determine the best one to downscale for wind data. Where the meteorological datasets are of the same type, the resolution of the global model forecasts and the data assimilation techniques used in their preparation can be used as criteria select candidate options for testing. The JMA JRA55, ECWMF ERA5 and NCEP GFS FNL will most likely probably gives some of the best downscaled wind speed data for this area in coastal Ghana, with the ERA5 being the most likely to be easily corrected, and therefore highly recommended in future tests and downscaling studies.

ACKNOWLEDGEMENTS

This work was supported through the project titled ‘Upgrading education and research capacity in Renewable Energy Technologies at Kwame Nkrumah University of Science and Technology (KNUST) Kumasi Ghana’, and funded by Norwegian Agency for Development Cooperation (Norad) through the Energy and Petroleum (EnPe) programme.

The JMA J55 dataset is from the Japanese 55-year Reanalysis (JRA-55) Project, carried out by the Japan Meteorological Agency (JMA).

TABLE OF ACRONYMS

3DVAR	Three-Dimensional Variational	ME	Mean Error
4DVAR	Four-Dimensional Variational	MODIS	Moderate Resolution Imaging Spectroradiometer
AGCM	Atmospheric Global Circulation Model	NCAR	National Centre for Atmospheric Research
ARW	Advanced Research WRF	NCEP	National Centres for Environmental Prediction
CC	Correlation Coefficient	NDVI	Normalized Difference Vegetation Index
CDF	Cumulative Density Function	NWP	Numerical Weather Prediction
ECWMF	European Centre for Medium-Range Weather Forecasts	PBL	Planetary Boundary Layer
EnKF	Ensemble Kalman Filter	RMSE	Root Mean Squared Error
EPS	Ensemble Prediction System	SODAR	Sound Detection and Ranging
GFS	Global Forecast System	STDE	Standard Deviation of the Error
GFS	Global Forecast System	UCAR	University Corporation for Atmospheric Research
GriB	Gridded Binary	USGS	United States Geological Survey
IGBP	International Geosphere Biosphere Program	WPD	Wind Power Density
JMA JRA	Japanese Meteorological Agency	WRF	Weather Research and Forecasting
LIDAR	Light Detection and Ranging	WRFDA	WRF Data Assimilation
LULC	Land Use and Land Cover		

APPENDIX

Table A1: Average predictions and error metrics at 40 m and 50 m.

	50 m											40 m											
	Average Wind Speeds (m/s)	RMSE (m/s)	STDE (m/s)	CC	ME (m/s)	Skill Score	<i>c</i>	<i>k</i>	Mean WPD (Wm ⁻²)	WPD Error (%)	Max CDF Error	Average Wind Speeds (m/s)	RMSE (m/s)	STDE (m/s)	CC	ME (m/s)	Skill Score	<i>c</i>	<i>k</i>	Mean WPD (Wm ⁻²)	WPD Error (%)	Max CDF Error	
Observation	6.79						7.5	4.2	220			6.70						7.4	4.2	212			
MODIS_CFSv2	5.97	1.68	1.46	0.61	-0.82	2.10	6.5	4.9	143	-35.1	0.23	5.82	1.73	1.49	0.58	-0.87	1.74	6.3	4.9	133	-37.3	0.25	
USGS_CFSv2	5.97	1.68	1.46	0.61	-0.83	2.13	6.5	4.7	144	-34.5	0.22	5.83	1.72	1.49	0.59	-0.87	1.81	6.4	4.8	134	-36.6	0.24	
MODIS_ERA5	5.68	1.61	1.16	0.77	-1.11	3.01	6.2	4.4	127	-42.1	0.28	5.58	1.62	1.17	0.76	-1.12	2.93	6.1	4.4	120	-43.2	0.28	
USGS_ERA5	5.70	1.60	1.17	0.76	-1.09	3.01	6.2	4.5	128	-42.0	0.28	5.58	1.63	1.18	0.75	-1.12	2.87	6.1	4.6	119	-43.6	0.29	
MODIS_ERA-I	5.77	1.64	1.28	0.72	-1.02	2.67	6.3	4.3	134	-39.0	0.25	5.72	1.60	1.27	0.71	-0.98	2.74	6.3	4.4	130	-38.4	0.25	
USGS_ERA-I	5.69	1.73	1.32	0.69	-1.11	2.25	6.3	4.2	129	-41.5	0.27	5.63	1.70	1.32	0.69	-1.07	2.31	6.2	4.3	125	-41.0	0.26	
MODIS_FNL	5.93	1.47	1.19	0.75	-0.86	3.40	6.5	4.8	141	-35.9	0.24	5.86	1.46	1.20	0.74	-0.84	3.38	6.4	4.9	135	-36.1	0.24	
USGS_FNL	5.87	1.49	1.17	0.76	-0.92	3.34	6.4	4.8	137	-37.9	0.25	5.79	1.49	1.18	0.75	-0.90	3.33	6.3	4.9	131	-38.1	0.25	
MODIS_JRA55	6.21	1.39	1.26	0.74	-0.58	3.69	6.8	4.2	169	-23.4	0.14	6.17	1.37	1.26	0.73	-0.53	3.70	6.8	4.3	164	-22.4	0.13	
USGS_JRA55	6.18	1.43	1.29	0.73	-0.62	3.51	6.8	4.2	166	-24.6	0.15	6.13	1.41	1.29	0.72	-0.57	3.52	6.7	4.3	161	-23.7	0.14	
MODIS_R2	5.57	2.11	1.72	0.52	-1.22	0.20	6.2	3.6	130	-41.1	0.27	5.50	2.09	1.71	0.52	-1.20	0.21	6.1	3.6	123	-41.7	0.27	
USGS_R2	5.46	2.15	1.68	0.54	-1.34	0.13	6.1	3.6	121	-44.9	0.30	5.37	2.13	1.67	0.53	-1.32	0.13	6.0	3.6	115	-45.6	0.30	

Table A2: Seasonal average predictions at 60 m and error metrics.

	September (in the Rainy Season)											February (Harmattan)											
	Average Wind Speeds (m/s)	RMSE (m/s)	STDE (m/s)	CC	ME (m/s)	Skill Score	<i>c</i>	<i>k</i>	Mean WPD (Wm ⁻²)	WPD Error (%)	Max CDF Error	Average Wind Speeds (m/s)	RMSE (m/s)	STDE (m/s)	CC	ME (m/s)	Skill Score	<i>c</i>	<i>k</i>	Mean WPD (Wm ⁻²)	WPD Error (%)	Max CDF Error	
Observation	7.42						8.1	5.3	270			6.32						7.0	3.7	186.4			
MODIS_CFSv2	6.07	1.75	1.11	0.73	-1.35	2.34	6.6	5.6	146	-45.9	0.38	6.14	1.53	1.44	0.63	-0.18	2.44	6.7	4.4	161.2	-13.5	0.07	
USGS_CFSv2	6.02	1.79	1.12	0.72	-1.40	2.21	6.5	5.3	144	-46.7	0.38	6.18	1.48	0.00	0.66	-0.14	2.71	6.8	4.3	165.1	-11.4	0.06	
MODIS_ERA5	5.91	1.82	1.02	0.77	-1.51	2.34	6.4	5.6	134	-50.3	0.43	5.62	1.36	1.76	0.80	-0.70	3.32	6.3	3.5	134.2	-28.0	0.15	
USGS_ERA5	5.88	1.85	1.03	0.77	-1.54	2.25	6.4	5.6	133	-50.9	0.44	5.73	1.27	1.12	0.81	-0.59	3.63	6.3	3.7	138.6	-25.7	0.13	
MODIS_ERA-I	6.00	1.86	1.20	0.69	-1.42	1.93	6.5	4.9	145	-46.3	0.37	5.62	1.47	0.00	0.75	-0.70	2.84	6.2	3.8	129.9	-30.3	0.16	
USGS_ERA-I	5.86	1.99	1.23	0.67	-1.56	1.54	6.4	4.8	136	-49.6	0.41	5.61	1.49	1.31	0.73	-0.71	2.72	6.2	3.8	129.0	-30.8	0.16	
MODIS_FNL	6.17	1.64	1.05	0.76	-1.25	2.72	6.6	6.0	151	-44.1	0.38	5.82	1.32	0.00	0.77	-0.50	3.35	6.4	4.0	141.5	-24.1	0.12	
USGS_FNL	6.04	1.70	1.00	0.79	-1.38	2.68	6.5	5.8	143	-47.1	0.40	5.83	1.30	1.20	0.78	-0.49	3.43	6.4	4.0	141.8	-23.9	0.12	
MODIS_JRA55	6.86	1.26	1.13	0.73	-0.56	3.67	7.4	5.5	211	-21.8	0.16	5.61	1.59	0.00	0.69	-0.71	2.30	6.2	3.7	130.7	-29.9	0.16	
USGS_JRA55	6.75	1.35	1.17	0.72	-0.68	3.36	7.3	5.2	203	-24.8	0.18	5.67	1.58	1.44	0.69	-0.65	2.33	6.3	3.7	134.8	-27.7	0.15	
MODIS_R2	6.23	2.09	1.72	0.40	-1.19	0.42	6.8	4.6	165	-39.0	0.30	5.03	2.21	0.00	0.54	-1.29	0.07	5.6	3.0	103.6	-44.4	0.27	
USGS_R2	6.08	2.13	1.66	0.41	-1.34	0.34	6.6	4.8	152	-43.7	0.34	4.96	2.22	1.76	0.55	-1.36	0.12	5.6	3.0	100.4	-46.2	0.28	

REFERENCES

- Available GRIB Datasets from NCAR. (2020). Retrieved from http://www2.mmm.ucar.edu/wrf/users/download/free_data.html
- Barker, D., Huang, X.-Y., Liu, Z., Auligné, T., Zhang, X., Rugg, S., . . . Chen, Y. (2012). The weather research and forecasting model's community variational/ensemble data assimilation system: WRFDA. *Bulletin of the American Meteorological Society*, 93(6), 831-843.
- Boadh, R., Satyanarayana, A. N. V., Rama Krishna, T. V. B. P. S., & Madala, S. (2016). Sensitivity of PBL schemes of the WRF-ARW model in simulating the boundary layer flow parameters for its application to air pollution dispersion modeling over a tropical station. *Atmósfera*, 29, 61-81. doi:10.20937/ATM.2016.29.01.05
- Breeze, P. (2019). Chapter 11 - Wind Power. In *Power Generation Technologies (Third Edition)* (pp. 251-273): Newnes.
- Carvalho, D., Rocha, A., Gómez-Gesteira, M., & Silva Santos, C. (2014). WRF wind simulation and wind energy production estimates forced by different reanalyses: Comparison with observed data for Portugal. *Applied energy*, 117, 116-126. doi:10.1016/j.apenergy.2013.12.001
- Chadee, X., Seegobin, N., & Clarke, R. (2017). Optimizing the Weather Research and Forecasting (WRF) Model for Mapping the Near-Surface Wind Resources over the Southernmost Caribbean Islands of Trinidad and Tobago. *Energies*, 10(7), 931. doi:10.3390/en10070931. (Accession No. doi:10.3390/en10070931)
- De Meij, A., & Vinuesa, J. F. (2014). Impact of SRTM and Corine Land Cover data on meteorological parameters using WRF. *Atmospheric Research*, 143, 351-370. doi:<https://doi.org/10.1016/j.atmosres.2014.03.004>
- Dee, D., Fasullo, J., Shea, D., Walsh, J., & , N. S. E. (2016, December 12, 2016). Atmospheric Reanalysis: Overview & Comparison Tables. Retrieved from <https://climatedataguide.ucar.edu/climate-data/atmospheric-reanalysis-overview-comparison-tables>
- Dee, D. P., Uppala, S., Simmons, A., Berrisford, P., Poli, P., Kobayashi, S., . . . Bauer, d. P. (2011). The ERA-Interim reanalysis: Configuration and performance of the data assimilation system. *Quarterly Journal of the Royal Meteorological Society*, 137(656), 553-597.
- Deserno, M. (2004). Linear and Logarithmic Interpolation. Retrieved from https://www.cmu.edu/biolphys/deserno/pdf/log_interpol.pdf
- Dzebre, D. E. K., Acheampong, A. A., Ampofo, J., & Adaramola, M. S. (2019). A sensitivity study of Surface Wind simulations over Coastal Ghana to selected Time Control and Nudging options in the Weather Research and Forecasting Model. *Heliyon*, 5(3), e01385. doi:<https://doi.org/10.1016/j.heliyon.2019.e01385>
- Dzebre, D. E. K., & Adaramola, M. S. (2019). Impact of Selected Options in the Weather Research and Forecasting Model on Surface Wind Hindcasts in Coastal Ghana. *Energies*, 12(19), 3670. doi:<https://doi.org/10.3390/en12193670>
- Dzebre, D. E. K., Ampofo, J., & Adaramola, M. S. (2021). An assessment of high-resolution wind speeds downscaled with the Weather Research and Forecasting Model for coastal areas in Ghana. *Heliyon*, 7(8), e07768. doi:<https://doi.org/10.1016/j.heliyon.2021.e07768>
- ECWMF. (2012). *ERA-Interim Project*. Retrieved from: <https://doi.org/10.5065/D6CR5RD9>

- Emery, C., Tai, E., & Yarwood, G. (2001). *Enhanced meteorological modeling and performance evaluation for two Texas ozone episodes*. Retrieved from
- Fernández-González, S., Martín, M. L., García-Ortega, E., Merino, A., Lorenzana, J., Sánchez, J. L., . . . Sanz Rodrigo, J. (2017). Sensitivity Analysis of the WRF Model: Wind-Resource Assessment for Complex Terrain. *Journal of Applied Meteorology and Climatology*, (2017). doi:10.1175/JAMC-D-17-0121.1
- Gbode, I. E., Dudhia, J., Ajayi, V. O., & Ogunjobi, K. O. (2017). Evaluation of Weather Research and Forecasting (WRF) model physics in simulating West African Monsoon (WAM). In: Presentation.
- Ghana Renewable Energy Master Plan Taskforce. (2019). *Ghana Renewable Energy Master Plan*. Retrieved from
- Ghati, S., & Mohan, M. (2015). The Impact of Land Use/Land Cover on WRF Performance in a Sub-Tropical Urban Environment. In: Presentation.
- Global Wind Energy Council. (2023). *GWEC Global Wind Report - 2023*. In.
- Gunwani, P., & Mohan, M. (2017). Sensitivity of WRF model estimates to various PBL parameterizations in different climatic zones over India. *Atmospheric Research*, 194, 43-65. doi:10.1016/j.atmosres.2017.04.026
- Hersbach, H., Bell, B., Berrisford, P., Biavati, G., Horányi, A., Muñoz Sabater, J., Nicolas, J., Peubey, C., Radu, R., Rozum, I., Schepers, D., Simmons, A., Soci, C., Dee, D., Thépaut, J.-N. (2018). *ERA5 hourly data on pressure levels from 1959 to present*. ERA5. Retrieved from: <https://cds.climate.copernicus.eu/cdsapp#!/home>
- Huang, X.-Y., Xiao, Q., Barker, D. M., Zhang, X., Michalakes, J., Huang, W., . . . Kuo, Y.-H. (2009). Four-Dimensional Variational Data Assimilation for WRF: Formulation and Preliminary Results. *Monthly Weather Review*, 137(1), 299-314. doi:10.1175/2008mwr2577.1
- Japan Meteorological Agency. (2013). *JRA-55: Japanese 55-year Reanalysis, Daily 3-Hourly and 6-Hourly Data*. Retrieved from: <https://doi.org/10.5065/D6HH6H41>
- Jiménez-Esteve, B., Udina, M., Soler, M., Pepin, N., & Miró, J. (2017). Land Use and Topography Influence in a Complex Terrain Area: A High Resolution Mesoscale Modelling Study over the Eastern Pyrenees using the WRF Model. *Volume 202*, 49-62. doi:10.1016/j.atmosres.2017.11.012
- Kalnay, E., Li, H., Miyoshi, T., Yang, S.-C., & Ballabrera-Poy, J. (2007). 4-D-Var or ensemble Kalman filter? *Tellus A*, 59(5), 758-773. doi:10.1111/j.1600-0870.2007.00261.x
- Lorenc, A. (2003). Relative Merits of 4D-Var and Ensemble Kalman Filter. Retrieved from ecmwf.org/sites/default/files/elibrary/2003/10817-relative-merits-4d-var-and-ensemble-kalman-filter.pdf
- McGuffie, K., & Henderson-Sellers, A. (2005). *A climate modelling primer*: John Wiley & Sons.
- Mughal, M. O., Lynch, M., Yu, F., McGann, B., Jeanneret, F., & Sutton, J. (2017). Wind modelling, validation and sensitivity study using Weather Research and Forecasting model in complex terrain. *Environmental Modelling & Software*, 90, 107-125. doi:10.1016/j.envsoft.2017.01.009
- National Centers for Environmental Prediction/National Weather Service/NOAA/U.S. Department of Commerce. (2000a). *NCEP FNL Operational Model Global Tropospheric Analyses, continuing from July 1999*. Retrieved from: <https://doi.org/10.5065/D6M043C6>

National Centers for Environmental Prediction/National Weather Service/NOAA/U.S. Department of Commerce. (2000b). *NCEP/DOE Reanalysis 2 (R2)*. Retrieved from: <http://rda.ucar.edu/datasets/ds091.0/>

Parker, W. S. (2016). Reanalyses and Observations: What's the Difference? *Bulletin of the American Meteorological Society*, 97(9), 1565-1572. doi:10.1175/bams-d-14-00226.1

Rabier, F., & Liu, Z. (2003). *Variational data assimilation: theory and overview*. Paper presented at the ECMWF Seminar on Recent developments in data assimilation for atmosphere and ocean.

Saha, S., Moorthi, S., Wu, X., Wang, J., Nadiga, S., Tripp, P., . . . Becker, E. (2014). The NCEP Climate Forecast System Version 2. *Journal of Climate*, 27(6), 2185-2208. doi:10.1175/jcli-d-12-00823.1

Saha, S., Moorthi, S., Wu, X., Wang, J., Nadiga, S., Tripp, P., . . . Becker, E. (2011). *NCEP Climate Forecast System Version 2 (CFSv2) 6-hourly Products*. Retrieved from: <https://doi.org/10.5065/D61C1TXF>

Santos-Alamillos, F. J., Pozo-Vázquez, D., Ruiz-Arias, J. A., & Tovar-Pescador, J. (2015). Influence of land-use misrepresentation on the accuracy of WRF wind estimates: Evaluation of GLCC and CORINE land-use maps in southern Spain. *Atmospheric Research*, 157, 17-28. doi:<https://doi.org/10.1016/j.atmosres.2015.01.006>

Schicker, I., Arnold Arias, D., & Seibert, P. (2016). Influences of updated land-use datasets on WRF simulations for two Austrian regions. *Meteorology and Atmospheric Physics*, 128(3), 279-301. doi:10.1007/s00703-015-0416-y

Warner, T. T. (2011). *Numerical weather and climate prediction*. Cambridge CB2 8RU, UK: Cambridge University Press.

Wei Wang, C. B., Michael Duda, Jimmy Dudhia, Dave Gill, Michael Kavulich, Kelly Keene, Ming Chen, Hui-Chuan Lin, John Michalakes, Syed Rizvi, Xin Zhang, Judith Berner, Soyoung Ha and Kate Fossell. (2016). ARW Version 3 Modeling System User's Guide. In. Colorado, USA: NCAR.

WRF V3 Geographical Static Data Downloads Page Page. (06/05/2018). Retrieved from http://www2.mmm.ucar.edu/wrf/users/download/get_sources_wps_geog_V3.html

Yang, J., & Duan, K. (2016). Effects of Initial Drivers and Land Use on WRF Modeling for Near-Surface Fields and Atmospheric Boundary Layer over the Northeastern Tibetan Plateau. *Advances in Meteorology*, 2016, 16. doi:10.1155/2016/7849249

Zhao, D.-M., & Wu, J. (2018). Evaluating the impacts of land use and land cover changes on surface air temperature using the WRF-mosaic approach. *Atmospheric and Oceanic Science Letters*, 11(3), 262-269. doi:10.1080/16742834.2018.1461527